B-meson production between the $\Upsilon(4S)$ and $\Upsilon(6S)$ and the possibility of detecting B-$\bar{B}$ mixing

Seiji Ono*
Institute of Physics, University of Tokyo, Komaba, Meguro-ku, Tokyo 153, Japan

A. I. Sanda
Rockefeller University, New York, New York 10021

N. A. Törnqvist
Department of Physics, Åbo Akademi, 20500 Åbo, Finland
and Department of High Energy Physics, University of Helsinki, 00170 Helsinki 17, Finland
(Received 3 December 1985)

A study is made of the quark-pair-creation model, the quarkonium-hybrid mixing model, and the unitarized quark model in connection with their ability to reproduce $R \equiv (\sigma_{\text{had}}/\sigma_{\mu\mu})$ between $\Upsilon(4S)$ and $\Upsilon(6S)$ and at the same time be consistent with all known facts about Γ and ψ systems. Models which passed the above test are used to compute all partial cross sections for pair production of B mesons. This result is used to estimate the rate for the B_d-$\bar{B}_d$ and B_s-$\bar{B}_s$ mixing effect as a function of the c.m. energy. Our result can be eventually used to search for new physics beyond the standard model.

I. INTRODUCTION

While the recently measured[1] value of ϵ'/ϵ is not yet evidence against the standard model, it can be taken as a hint that a deviation from the standard model[2] is in the horizon. A heavier than expected top-quark mass or observation of peculiar events at $p\bar{p}$ colliders would further encourage this line of thought. Supersymmetric partners of quarks, gluons, and gauge bosons may not be hopelessly heavy, or there may be a fourth family of quarks and leptons.

We may be treated to surprises as experimental results from $p\bar{p}$ colliders at CERN, Tevatron at Fermilab, TRISTAN at KEK, LEP at CERN, and HERA at DESY become available.

A study of B-$\bar{B}$ mixing[3-5] is an alternative approach to search for new physics. A detailed study of this quantum-mechanical effect will yield information on the properties of particles which are too heavy to be produced at any of the accelerators to be completed in the near future. A case in point is the study of K^0-$\bar{K}^0$ mixing, which provided the key to formulating the standard model.

A first-round theoretical study of B-$\bar{B}$ mixing is now completed.[6] The standard model predicts large B_s-$\bar{B}_s$ mixing (B_q denotes $b\bar{q}$ bound state) and a large CP-violating asymmetry for B_d decays. Furthermore, there is an indication that it is easier to estimate the hadronic matrix elements. We remind the reader that the ambiguity in estimating K-meson matrix elements forbids us to draw definite conclusions on the validity of the standard model based on the new experimental result for ϵ'/ϵ.

The first step toward the search for new physics along this direction is the discovery of B-$\bar{B}$ mixing. In this article we shall address this question.

One way to observe B-$\bar{B}$ mixing is to produce a "B beam" in fixed-target machines. This has been discussed[7] as a possibility at the Superconducting Super Collider (SSC). For now we shall concentrate on the possibility of observing B-$\bar{B}$ mixing in the Υ region where B mesons are produced nearly at rest and thus there is a tight control on the final-state composition.

In order to predict the B-$\bar{B}$ mixing effect, we need a model which can be used to compute all partial production cross sections. A first check on the model is to compare the prediction for the total section with the experimentally measured cross section.

The energy region between $\Upsilon(4S)$ and $\Upsilon(6S)$ has been studied experimentally by the CUSB[8] and CLEO[9] groups. There are two features of the data which are very difficult to understand[10-12] within the context of a simple potential model: (i) The mass splitting between $\Upsilon(5S)$ and $\Upsilon(4S)$ is larger than that between $\Upsilon(4S)$ and $\Upsilon(3S)$, and (ii) there are indications of resonancelike structures just above $\Upsilon(4S)$. One can consider various possibilities to explain these anomalies. We mention two of them.

(i) The quarkonium-hybrid-mixing (QHM) model.[10-12] The structure just above $\Upsilon(4S)$ corresponds to the mixing partner of $\Upsilon(4S)$ and contains mainly $b\bar{b}g$. Because of mixing the energy level of $\Upsilon(4S)$ is pushed down.

(ii) The unitarized quark model (UQM).[13-15] Because of unitarity effects the spacing between $\Upsilon(4S)$ and $\Upsilon(5S)$ increases. The structure just above $\Upsilon(4S)$ corresponds to the openings of $B\bar{B}^*, B^*\bar{B}^*$ channels and a small "background" from all the other upsilon states.

In the present paper we will use mainly the QHM model to study $B\bar{B}$ mixing effects.

The plan of this paper is as follows. In Sec. II we define the mixing parameters which we study. In Sec. III we will briefly explain the $b\bar{b}$-$b\bar{b}g$ mixing model and show

how to reproduce $R \equiv \sigma_{\text{had}}/\sigma_{\mu\mu}$. As a second model we use the unitarized quark model to reproduce R in Sec. IV. Using these models we compute $B\bar{B}$ mixing effects in Sec. V. More detailed descriptions of the quark-pair-creation (QPC) model, the QHM model, and the UQM are given in Appendix A. We show in Appendix B $B(\Upsilon(4S) \rightarrow B^+B^-)/B(\Upsilon(4S) \rightarrow B^0\bar{B}^0) = 0.4984/0.5016$ for $B^0 - B^{\pm} = 4$ MeV. Finally we make comments on the observability of CP violation in Appendix C.

II. MIXING PARAMETERS[4,16]

The parameter which governs the mixing is denoted by $x = 2\Delta m/\Gamma$ which is the ratio of the lifetime to the time required for mixing. The predictions of x_d and x_s corresponding to the parameter x for B_d and B_s mesons, respectively, can be given in terms of the constants β_d and β_s:

$$x_d = \beta_d(0.05\text{–}0.2), \quad x_s = \beta_s \times 1.6 . \tag{2.1}$$

The constants are estimated to be

$$\begin{aligned} &\beta_d = 1, 0.40, 0.32, 0.33 , \\ &\beta_s = 1, 0.54, 0.54, 0.48 , \end{aligned} \tag{2.2}$$

for the vacuum-saturation approximation, harmonic-oscillator model, relativistic harmonic oscillator model, and bag model, respectively. One expects that the potential model description for the B meson should be better than that for the K meson due to the larger b-quark mass. This is probably the reason behind the fact that β is fairly model independent.

The B_q-$\bar{B}_q$ mixing can be observed by detecting dilepton events:

$$\begin{array}{l} e^+e^- \rightarrow B_q\bar{B}_q + X \\ \qquad\quad \big\lfloor \rightarrow B_q \rightarrow \mu^- \bar{\nu}_\mu c \\ \qquad\quad \rightarrow \mu^- \bar{\nu}_\mu c \end{array} \tag{2.3}$$

or its charge-conjugate reaction. Here B_q denotes either B_d or B_s. Obviously $\mu^-\bar{\nu}_\mu$ can be replaced by $e^-\bar{\nu}_e$.

In the Υ region, B's are produced in the combination

$$B_q\bar{B}_q, \quad B_q\bar{B}_q^* + \text{c.c.}, \quad B_q^*\bar{B}_q^* , \tag{2.4}$$

where $q = d$ or s. From the decay $B^* \rightarrow B + \gamma$, it is obvious that $B_q\bar{B}_q$ produced from $B_q\bar{B}_q^*$ is in an even l-wave state while all other channels result in an odd l-wave state.

The probability of same-sign dilepton events produced per initial $B_q\bar{B}_q$ pairs depend on l as[4]

$$\begin{aligned} P_{q,1} &\equiv \tfrac{1}{4}(N_q^{++} + N_q^{--})_{l=\text{odd}} = \frac{1}{2}\frac{x_q^2}{1+x_q^2} , \\ P_{q,0} &\equiv \tfrac{1}{4}(N_q^{++} + N_q^{--})_{l=\text{even}} = \frac{1}{2}\frac{3x_q^2 + x_q^4}{(1+x_q^2)^2} , \end{aligned} \tag{2.5}$$

where the subindex 0 or 1 stands for even or odd l, respectively. For all values of x_q, $P_{q,0} > P_{q,1}$. This suppression of $P_{q,l}$ for odd l compared to even l follows from the Bose statistics which forbids having B_qB_q or $\bar{B}_q\bar{B}_q$ for odd l at any instant of time.

It is convenient to define the signal as the same-sign dilepton cross section divided by the $e^+e^- \rightarrow \mu^+\mu^-$ cross section and the square of the semileptonic branching ratio of B_s (R_s)

$$\begin{aligned} S = \frac{\sigma^{++} + \sigma^{--}}{\sigma_{\mu^+\mu^-} R_s^2} = \left[\frac{R_d}{R_s}\right]^2 &[\Delta R(B_d\bar{B}_d + B_d^*\bar{B}_d^*)P_{d,1} + \Delta R(B_d\bar{B}_d^* + \text{c.c.})P_{d,0}] \\ &+ [\Delta R(B_s\bar{B}_s + B_s^*\bar{B}_s^*)P_{s,1} + \Delta R(B_s\bar{B}_s^* + \text{c.c.})P_{s,0}] . \end{aligned} \tag{2.6}$$

Currently there is no detailed knowledge of the individual semileptonic branching ratios R_q of the B_q mesons. In principle, the ratio $(R_d/R_s)^2$ can range, say, from 0.5 to 2.

The ratio of equal-sign dilepton events $\sigma^{++} + \sigma^{--}$ to opposite-sign dilepton events σ^{+-} (we call this the E/O ratio) depends on the angular momentum of $B_q\bar{B}_q$:

$$\begin{aligned} R^q_{l=1} &= \frac{\sigma^{++} + \sigma^{--}}{\sigma^{+-}} = \frac{x_q^2}{2 + x_q^2} , \\ R^q_{l=0} &= \frac{3x_q^2 + x_q^4}{2 + x_q^2 + x_q^4} . \end{aligned} \tag{2.7}$$

III. MODEL PREDICTIONS FOR B- AND B_s-MESON PRODUCTION BETWEEN $\Upsilon(4S)$ AND $\Upsilon(6S)$

We have studied several models to understand B-meson production between the $\Upsilon(4S)$ and $\Upsilon(6S)$. In this section we will try to reproduce R in this energy region by model calculations.

It is widely accepted that the quark-pair-creation (QPC) model[17] gives a reasonable description for decay processes allowed by the Okubo-Zweig-Iizuka (OZI) rule. The contribution to R from the process $\Upsilon(nS) \rightarrow X$ ($X = B\bar{B}, B\bar{B}^* + \text{c.c.}, \ldots$) is given by[18]

$$\Delta R = \frac{3\pi^2}{2k^2}\Gamma_{ee}(nS)\frac{\pi^{-1}\omega_0\Gamma(\omega)^X}{(\omega_0^2 - \omega^2)^2 + \omega_0^2[\Gamma(\omega)^{\text{total}}]^2}\frac{d\omega^2}{\sigma_{\mu\mu}} , \tag{3.1}$$

$$\Gamma^{\text{total}} = \sum_{X = B\bar{B}, B\bar{B}^*, \ldots} \Gamma^X, \quad \sigma_{\mu\mu} = \frac{4\pi\alpha^2}{3(2k)^2}, \quad 2k = \omega .$$

We compute the OZI-rule-allowed width $\Gamma(\omega)^X$ in the QPC model. The model which we use here is identical with the one in Ref. 18 except that we neglect the beam width and radiative corrections which are unimportant for

broad resonances. In our model the main adjustable parameter is γ_{QPC}, the pair-creation strength.

We have found that the QPC model with universal γ_{QPC} is not very successful to reproduce all OZI-rule-allowed widths for ψ and Υ states above threshold. Also the structure in R between $\Upsilon(4S)$ and $\Upsilon(5S)$ seems to require either more resonances than those predicted by the potential model or a new mechanism for higher smooth background above the $B\bar{B}$ threshold.

There are further difficulties in the potential model. (i) The mass of $\psi(4.03)$ is lower than a typical theoretical estimate for $(c\bar{c})_{3S}$ by around 70 MeV. (ii) We expect $\Gamma_{ee}(2D)/\Gamma_{ee}(3S)\sim\frac{1}{20}$ while the experimental value of this ratio is as large as one. (iii) The theoretical value of $\Gamma_{ee}(3S)$ is larger than the measured one by a factor 2.

The situation can be remedied systematically by postulating hybrid states $c\bar{c}g$ and $b\bar{b}g$, in which a gluon is included as a constituent particle. An impressive improvement can be made by replacing the conventional assignments $\psi(4030)=(c\bar{c})_{3S}$ and $\psi(4159)=(c\bar{c})_{2D}$ by the mixture states:

$$\psi(4030)\simeq\frac{1}{\sqrt{2}}[(c\bar{c})_{3S}+c\bar{c}g]\ ,$$
$$\psi(4159)\simeq\frac{1}{\sqrt{2}}[(c\bar{c})_{3S}-c\bar{c}g]\ . \tag{3.2}$$

The anomalies in $\Gamma_{ee}(2D)/\Gamma_{ee}(3S)$ and $\Gamma_{ee}(3S)$ are removed immediately by noticing that $c\bar{c}g$ does not couple to e^+e^-. Because of the mixing between $(c\bar{c})_{3S}$ and $c\bar{c}g$ one energy level is pushed down; thus, we can understand the unexpectedly low mass of $\psi(4030)$.

The assumption of the $c\bar{c}g$ state in this energy region is supported by the model calculations[19,21] which predict the lowest $c\bar{c}g$ state around $\psi(3S)$. In the Υ sector such models also predict the lowest $b\bar{b}g$ state just above $\Upsilon(4S)$. On the other hand, a typical potential model predicts a larger mass of $\Upsilon(4S)$ and larger $\Gamma_{ee}(4S)$ than the measured ones. Thus, it was speculated[10] that there might be $\Upsilon(4S)$-$b\bar{b}g$ mixing and the mixing partner might be found just above $\Upsilon(4S)$.

The possible candidate for the mixing partner was indeed found later just above $\Upsilon(4S)$ by both the CLEO[9] and CUSB[8] groups. However, some peaks in this energy region may be attributed to the opening of $B\bar{B}^*, B^*\bar{B}^*$ thresholds. In order to make the situation clearer we first compute ΔR as a function of energy is the QPC model without introducing $b\bar{b}$-$b\bar{b}g$ mixing. We assume $\Gamma_{ee}(4S)=0.26$, $\Gamma_{ee}(5S)=0.34$, $\Gamma_{ee}(6S)=0.28$, $\Gamma_{ee}(7S)=0.2$ keV. The result is compared with experimental data in Fig. 1. From this figure one finds that the structure between $\Upsilon(4S)$ and $\Upsilon(5S)$ is not enough to explain by the opening of various thresholds $B\bar{B}^*, B^*\bar{B}, B^*\bar{B}^*$. Next we compute ΔR by including $b\bar{b}$-$b\bar{b}g$ mixing. The results are shown in Fig. 2. The fit is clearly improved.

We call this model "the quarkonium-hybrid-mixing (QHM) model." This model will be used to compute various effects later. Using the QHM model we also compute ΔR from $B_d\bar{B}_d, B_d\bar{B}_d^*+\text{c.c.}, B_d^*\bar{B}_d^*$, and from $B_s\bar{B}_s, B_s\bar{B}_s^*+\text{c.c.}, B_s^*\bar{B}_s^*$, which are shown in Figs. 3 and 4, respectively.

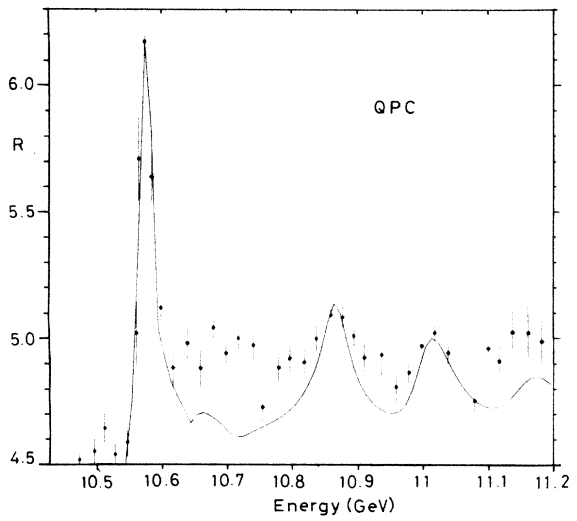

FIG. 1. The data on R from CLEO (Ref. 9) compared with the QPC model.

If the wave function of the B_s state is the same as that of the B_d (or B_u) state we must find the relation $\sigma(B_s\bar{B}_s)=\sigma(B_d\bar{B}_d)=\sigma(B_u\bar{B}_u)$. From Figs. 3 and 4 one can see that the $B_s\bar{B}_s$ production rate is less than that of $B_d\bar{B}_d$. This fact is used, e.g., in the recent analysis by the CUSB group.[22] The difference in the production rate is caused by the difference of the wave functions between B_d and B_s mesons. The wave function of the B_s meson in the momentum space is more spread out than that of the B_d meson because of the larger reduced mass. Therefore, the overlap integral $I(k)$ becomes smaller for the B_s meson than for the B_d meson due to the larger cancellations in the integral. This is the reason of the larger SU(3) breaking.

We will present more details about the QHM model in Appendix A.

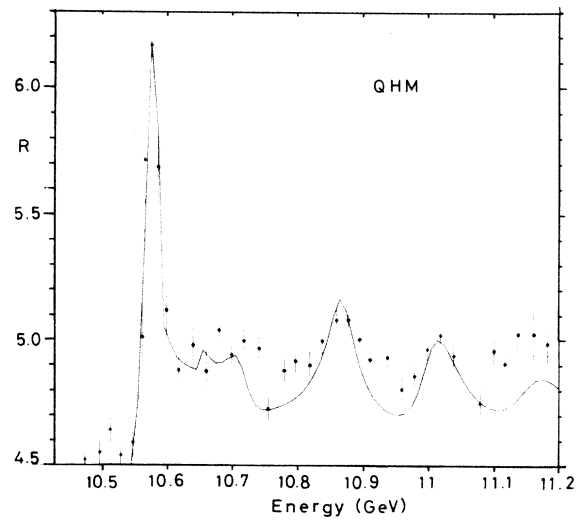

FIG. 2. Same as Fig. 1 but with the QHM model.

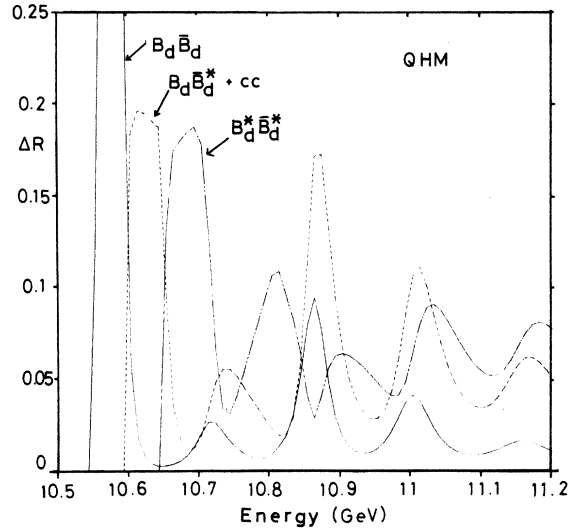

FIG. 3. The contribution to R from $B_d\bar{B}_d$, $B_d\bar{B}_d^*$+c.c., $B_d^*\bar{B}_d^*$ as predicted by the QHM model.

IV. THE UNITARIZED QUARK MODEL (UQM)

As is well known in nuclear-reaction theory (see, e.g., Ref. 23) the presence of coupled channels shifts the masses, introduces mixings between resonance states, and distorts the cross section from naive expectations. Since the couplings to channels allowed by the OZI rule are large the predictions of the naive quark model can be substantially modified in a more complete theory. In order to study these effects systematically we use the UQM, which was described in more detail previously.[13–15] One assumes that the Hamiltonian can be decomposed as

$$H=\begin{bmatrix} H_{Q\bar{Q}} & 0 \\ 0 & H_{\rm kin} \end{bmatrix}+\begin{bmatrix} 0 & H_{\rm QPC} \\ H_{\rm QPC} & 0 \end{bmatrix}, \tag{4.1}$$

where the two sectors of Hilbert space are the confined $Q\bar{Q}$ states and the continuum two meson states (e.g., $B\bar{B}$, $B\bar{B}^*$, etc.). The part $H_{Q\bar{Q}}$ is the naive quark-model Hamiltonian, while $H_{\rm kin}$ contains only a kinetic term for the two-meson sector and $H_{\rm QPC}$ describes the quark-pair-creation (QPC or $^3P_0$) model.[17]

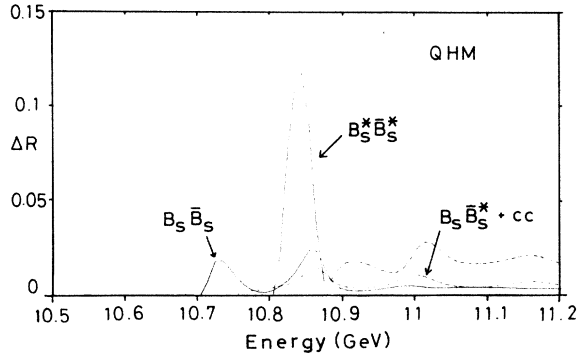

FIG. 4. Same as Fig. 3 but from $B_s\bar{B}_s$, $B_s\bar{B}_s^*$+c.c., $B_s^*\bar{B}_s^*$.

Using relativistic kinematics the physical masses and widths are given by the eigenvalues of a mass matrix $M^2(s)$, whose imaginary part is given by unitarity

$$\mathrm{Im}M_{ij}^2(s)=-\gamma_{\rm QPC}^2\sum_{CD}\mathcal{G}_{i,CD}(s)\mathcal{G}_{j,CD}(s)\ , \tag{4.2}$$

where the functions $\mathcal{G}_{i,CD}(s)$ are given by the QPC model and phase space $\rho_{CD}(s)$:

$$\gamma_{\rm QPC}\mathcal{G}_{i,CD}(s)=\langle i\mid H_{\rm QPC}\mid CD\rangle\rho_{CD}^{1/2}(s)\ . \tag{4.3}$$

The real part of M^2 is composed of the eigenvalues of the naive model (bare mass) and a mass shift term

$$\mathrm{Re}M_{ij}^2(s)=M_{i,\rm bare}^2\delta_{ij}-\frac{P}{\pi}\int_{s_{th}}^{\infty}\frac{\mathrm{Im}M_{ij}^2(s')}{s-s'}ds'\ . \tag{4.4}$$

The unitarity partial-wave amplitudes between channels $B\bar{B}$,$B\bar{B}^*$, etc., can then be written

$$T_{AB\to CD}(s)=\gamma_{\rm QPC}^2\sum_{i,j}\mathcal{G}_{i,AB}(s)[M_{ij}^2(s)-s]^{-1}\mathcal{G}_{j,CD}(s)\ . \tag{4.5}$$

For the e^+e^- channel the corresponding $\mathcal{G}_{i,e^+e^-}(s)$ is defined as in Eq. (4.3), but with $\langle i\mid H_{\rm QPC}\mid CD\rangle$ replaced by a constant. Because of the smallness of this coupling the e^+e^- channel can be neglected in the unitarity sum Eq. (4.2).

The simpler nonunitarized model discussed in the previous section can be considered as an approximation where (i) off-diagonal matrix elements of M_{ij}^2 are neglected and put equal to zero, (ii) the function $\mathrm{Re}M_{ii}(s)$ is replaced by constants absorbed into the bare masses, but $\mathrm{Im}M_{ii}(s)$ is kept unchanged, and (iii) interference terms between the resonances obtained in $\mid T\mid^2$ are neglected.

Sometimes the unitarization modifies dramatically naive expectations, in particular when the resonances are broad. But narrow resonance widths can also change substantially due to the mixing induced through the off-diagonal matrix elements of M_{ij}^2. An example is the Υ(4S) width which is reduced by almost a factor of 2.

The greatest uncertainty in the UQM comes from the matrix elements of $H_{\rm QPC}$ evaluated far off resonance for large s. Through the dispersion relation of Eq. (4.4) this means that $\mathrm{Re}M_{ij}(s)$ could be modified by a nearly constant piece. Thus the absolute value of a mass shift is more uncertain than a relative mass splitting like Υ(5S)-Υ(4S). Therefore, in Table I we show the mass shifts relative to the 5S. The uncertainty in the off-diagonal matrix elements of $\mathrm{Re}M_{ij}^2$ means that the mixing induced by the model could be incorrectly described. In Fig. 11(a) we compare the UQM with measurement of R. In Figs. 11(b) and 11(c) we show individual contributions to R from $B\bar{B}$,$B\bar{B}^*$, . . . , respectively. The result for S is given in Fig. 12. Further discussion of the details of the fit is in Appendix A 3.

V. $B\bar{B}$ mixing effects

In Sec. III we have shown that the QHM model can reproduce R between Υ(4S) and Υ(6S) well. Using this model we compute the quantity S of Eq. (2.6). The result

TABLE I. The parameters of the UQM calculation, i.e., resonance physical mass shift. The D-wave masses in parentheses are the approximate naive quark-model expectation to which the R of Fig. 11(a) is insensitive. The computed mass shifts from bare masses are given in the last column and are computed using the bare $\gamma_{\rm QPC}=3.029$.

State	Physical mass (GeV)	$\Gamma_{ee}^{\rm bare}(nS)$ (keV)	Calculated mass shift relative to $5S$ (MeV)
$1S$	9.460	1.26	−25.9
$2S$	10.0214	0.71	−52.9
$1D$	(~10.03)	0	−47.1
$3S$	10.353	0.52	−63.3
$2D$	(~10.41)	0	−64.4
$4S$	10.5775	0.41	−70.2
$3D$	(~10.63)	0	−65.6
$5S$	10.880	0.34	0 (Defn.)
$4D$	(~10.95)	0	−32.6
$6S$	11.009	0.26	−10.6
$5D$	(~11.07)	0	−8.6
$7S$	11.147	0.22	−3.6
$6D$	(~11.20)	0	5.3

is shown in Fig. 5, where $(R_s/R_d)=1$ is assumed. We consider four cases: (i) $x_d=0.2$, $x_s=1.6$; (ii) $x_d=0.1$, $x_s=1.3$; (iii) $x_d=0.05$, $x_s=1.0$; (iv) $x_d=0.016$, $x_s=0.77$.

The peak observed in Fig. 5 around $\Upsilon(5S)$ is dominated by events through $B_s\bar{B}_s$ at $\sqrt{s}=10.87$ GeV. For this reason the peak value of S varies very little ($<1\%$) for $0.5<(R_d/R_s)^2<2$.

Once the same-sign dilepton signal is observed experimentally at the $5S$ peak one can determine x_s from Fig. 5. The fraction of the signal which comes from $B_s\bar{B}_s$ is plotted in Fig. 6. From this figure one can see that the contribution from $B_s\bar{B}_s$ is more than 90% at $\Upsilon(5S)$.

The value of x_s is closely related to the top-quark mass.[16] The relation is plotted in Fig. 7. In Fig. 8 we also plot the E/O ratio $(\sigma^{++}+\sigma^{--})/\sigma^{+-}$ given in Eq. (2.7).

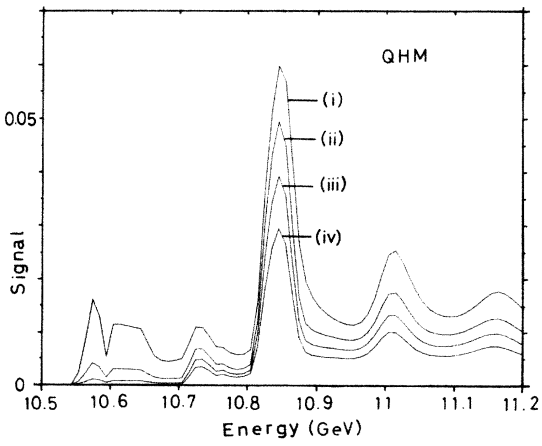

FIG. 5. The predicted signal S [Eq. (2.6)] using QHM model for four cases; (i) $x_d=0.2$, $x_s=1.6$; (ii) $x_d=0.1$, $x_s=1.3$; (iii) $x_d=0.05$, $x_s=1.0$; (iv) $x_d=0.016$, $x_s=0.77$. $R_s=R_d$ is assumed.

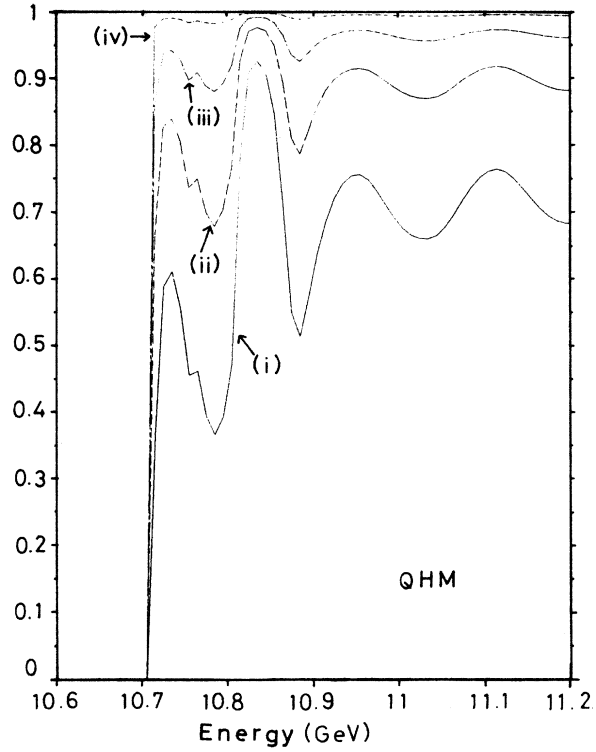

FIG. 6. The fraction of the same-sign dilepton signal which comes from $B_s\bar{B}_s$, i.e., $P(B_s\bar{B}_s\to l^{\pm}l^{\pm})/[P(B_s\bar{B}_s\to l^{\pm}l^{\pm})+P(B\bar{B}\to l^{\pm}l^{\pm})]$. It is assumed that every signal comes from either $B_d\bar{B}_d$ or $B_s\bar{B}_s$. The QHM model is used.

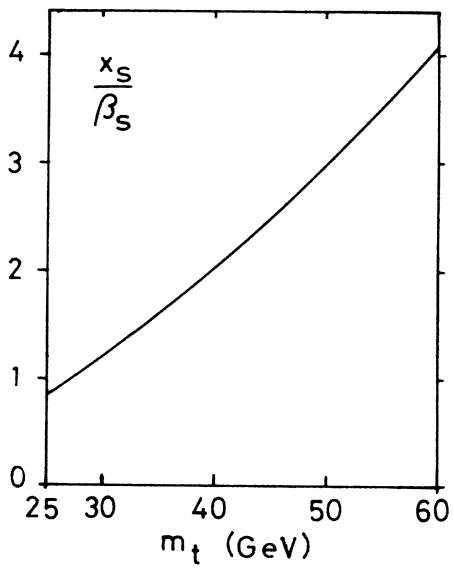

FIG. 7. x_s/β_s as a function of the top-quark mass. This quantity is given by $8.6\,U_2$ where U_2 is computed in Ref. 16. β_s is given in Eq. (2.2).

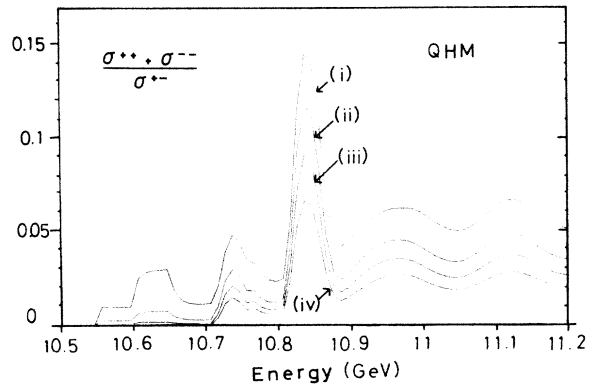

FIG. 8. The ratio $(\sigma^{++}+\sigma^{--})/\sigma^{+-}$ given in Eq. (7) as a function of energy predicted by the QHM model.

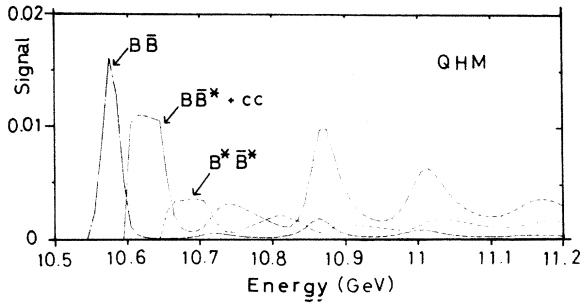

FIG. 9. The signal S [Eq. (2.6)] coming from $B\bar{B}$, $B\bar{B}^*$+c.c., and $B^*\bar{B}^*$ for $x_d=0.2$, $x_s=1.6$ in the QHM model.

The flat region in this ratio around 10.56 GeV corresponds to the Υ(4S) peak where only $B_d\bar{B}_d$ is produced; thus, the E/O ratio becomes constant $(=x_q^2/[2(1+x_q^2)])$. Just above the Υ(4S) region, i.e., $10.6<E<10.64$ GeV, the E/O ratio becomes about three times as much as that on Υ(4S) peak since the contribution from $B_d\bar{B}_d$+c.c. becomes important. However, as seen from Fig. 5 the dilepton production rate is not very large since the production rate of $B\bar{B}^*$+c.c. is about $\frac{1}{4}$ that of $B\bar{B}$ at Υ(4S). The situation will be the same for the peak at around 10.73 GeV. The E/O ratio becomes maximum around Υ(5S), which also corresponds to the maximum in the like-sign dilepton rate.

In Figs. 9 and 10 the signals S [Eq. (2.6)] coming from $B\bar{B}$, $B\bar{B}^*$+c.c., $B^*\bar{B}^*$, $B_s\bar{B}_s$, $B_s\bar{B}_s^*$+c.c., $B_s^*\bar{B}_s^*$ are plotted separately.

Comparing Fig. 5 (QHM model) with Fig. 12 (UQM) we see that both models predict similar results. Let us discuss in detail more about the signal from Υ(5S). We should first mention that the peak position of Υ(5S) resonance does not necessarily correspond to the maximum of the signal S, because the overlap in our model is a rapidly changing function. In the QHM model, e.g., the peak position in S is lower than the resonance peak position by around 20 MeV (this is the model-dependent result). The ratio

$$r_s \equiv \frac{B(\Upsilon(5S)\to B_s\bar{B}_s, B_s\bar{B}_s^*+\text{c.c.}, B_s^*\bar{B}_s^*)}{B(\Upsilon(5S)\to B\bar{B}, B\bar{B}^*, \ldots)+B(\Upsilon(5S)\to B_s\bar{B}_s, B_s\bar{B}_s^*, \ldots)} \tag{5.1}$$

is 0.1—0.2 at the Υ(5S) resonance peak. If we go down 20 MeV from the peak position, r_s increases to 0.3. At the Υ(5S) peak $r_s\sim 0.39$ in the UQM. According to the calculation by Lee-Franzini[5] who used the Cornell coupled-channel model[24] r_s is around 0.35 at Υ(5S) peak.

Although the UQM predicts a higher branching ratio into $B_s\bar{B}_s, B_s\bar{B}_s^*, \ldots$ than the QHM model, it assumes a lower leptonic width Γ_{ee}; thus the signal S is about the same as that of the QHM model. The difference in $\Gamma_{ee}(5S)$ comes from the assumption of the continuum background level in R $(=\sigma_{\text{had}}/\sigma_{\mu\mu})$ above threshold in both models.

Therefore, besides the values of x_s and x_d there are two kinds of ambiguities in the prediction of the signal rate S at (or near) Υ(5S): (i) theoretical ambiguity in $r_s\approx\pm 15\%$, and (ii) the error in the experimental value of $\Gamma_{ee}(5S)$, which is related to the level of continuum background. If a more precise value of $\Gamma_{ee}(5S)$ is found experimentally in the future one can easily recalculate S by multiplying $\Gamma_{ee}^{\text{new}}/\Gamma_{ee}^{\text{here}}$.

VI. CONCLUSION

We have estimated the $B_q\bar{B}_q, B_q\bar{B}_q^*$+c.c., $B_q^*\bar{B}_q^*$ production cross section using the quarkonium-hybrid mixing

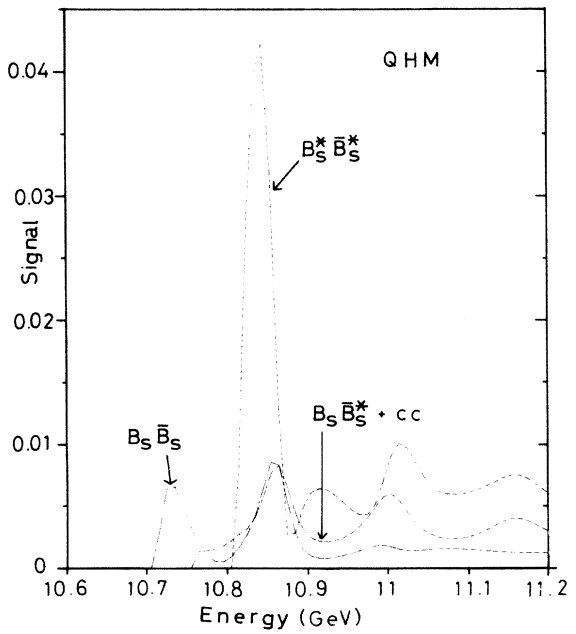

FIG. 10. Same as Fig. 9 but for $B_s\bar{B}_s$, $B_s\bar{B}_s^*$+c.c., and $B_s^*\bar{B}_s^*$.

model and unitarized quark model. While the detail dynamics of these models vary, they predict comparable production cross sections above threshold.

It has been shown that around one-third of $\Upsilon(5S)$ decay consists of $B_s\bar{B}_s$, $B_s\bar{B}_s^*+$c.c., and $B_s^*\bar{B}_s^*$. This presents us with a possibility of "dialing" B_d or B_s choosing to run on $\Upsilon(4S)$ or $\Upsilon(5S)$.

It is seen from Figs. 2 and 11 that the $B_s\bar{B}_s$,$B_s\bar{B}_s^*$ +c.c.,$B_s\bar{B}_s^*$ production cross section at $\Upsilon(5S)$ is about $\frac{1}{10}$ that of $B_d\bar{B}_d$ at $\Upsilon(4S)$. In spite of this disadvantage in rate, the number of dileptons expected from B_q-$\bar{B}_q$ mixing is expected to be larger at $\Upsilon(5S)$ than at $\Upsilon(4S)$ as seen Figs. 4 and 12. This is due to expected large B_s-$\bar{B}_s$ mixing.

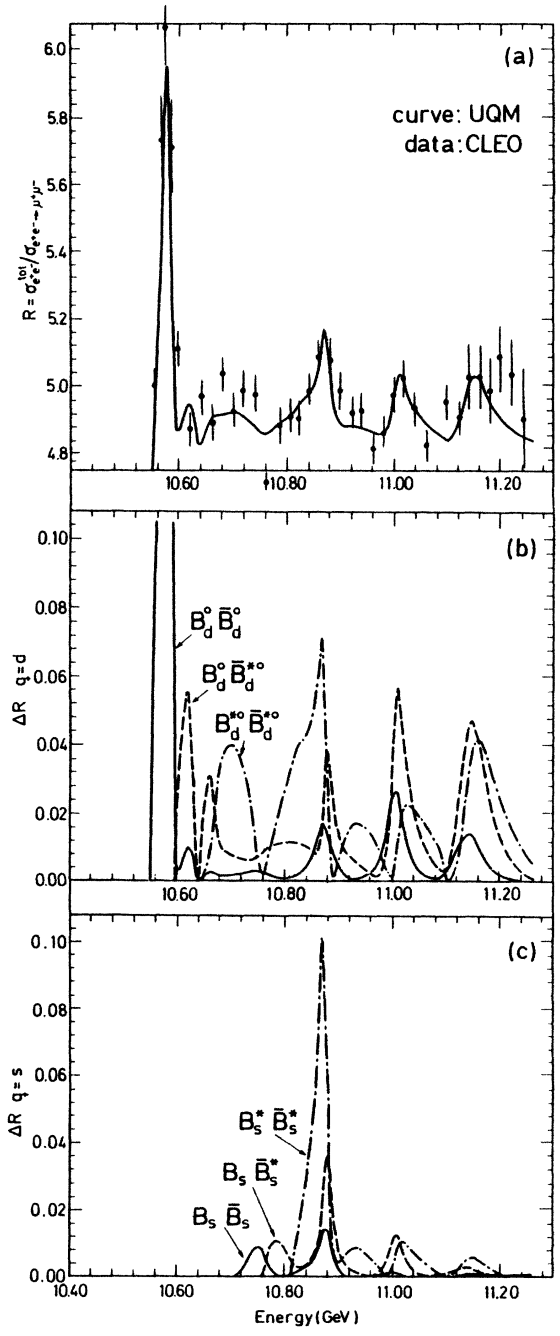

FIG. 11. Same as Figs. 2–4 but for UQM.

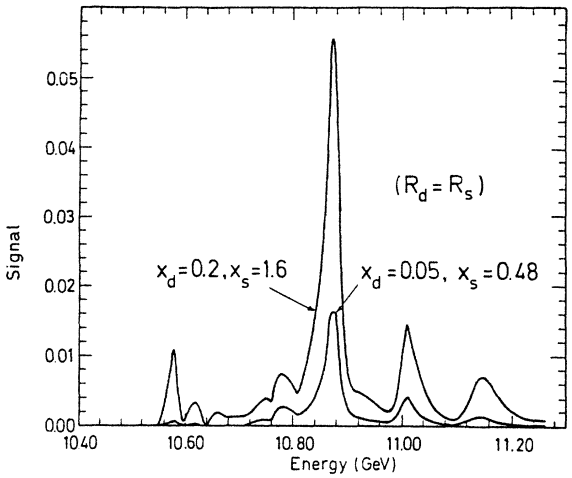

FIG. 12. Same as Fig. 5 but for UQM.

There are several uncertainties in our computation besides those shown in Eqs. (2.1) and (2.2).

(1) We estimate the uncertainties in the computed production cross section to be ±15% at $\Upsilon(5S)$, where the uncertainties in $\Gamma_{ee}(5S)$ are not included. Note that CLEO[9] and CUSB[8] found $\Gamma_{ee}(5S)=0.22\pm0.12$ and 0.365 ± 0.070 keV, respectively.

(2) The values of x_d and x_s Eq. (2.1) is for $m_t\sim35$ GeV. Roughly, x varies as m_t^2 and the dilepton rate varies as m_t^4 for small x.

Once the mixing is established, m_t can be predicted from Fig. 7. It is of major importance to check our prediction against experiment. Disagreement beyond experimental and theoretical error will be a signal for new physics.

Finally we remind the reader that we concentrated on events with leptonic final states given in (2.3). It is obvious that our analysis holds for events with reconstructed B mesons provided that the final state leads to the identification of its parent.

ACKNOWLEDGMENTS

We would like to thank H. Aihara, I. I. Bigi, T. Kamae, O. Pene, S. Yazaki, and K. Yazaki for discussions. Two of the authors (A.I.S. and N.A.T.) wish to thank Keiji Igi for the kind hospitality extended to them during their visit to the University of Tokyo where this work was brought into its final form. The other author (S.O.) also wishes to thank Soryushi Shogakukai for financial support. The computer calculation for this work has been financially supported in part by the Institute for Nuclear Study, University of Tokyo.

APPENDIX A: THE MODELS

1. QPC Model

We present here more details about our fitting procedure to R. In the QPC model a free parameter is a coupling constant $\gamma_{\rm QPC}$ which describes the strength of the

pair creation. We have failed to find a suitable universal value for $\gamma_{\rm QPC}$ to produce widths for the $\Upsilon(4S)$, $\Upsilon(5S)$, and $\Upsilon(6S)$ simultaneously. Therefore, we keep our previous coupling constant $\gamma_{\rm QPC}=2.8$ only for $\Upsilon(4S)$ while $\Upsilon_{\rm QPC}=5.6$ for higher states. This means we assume that $\Upsilon(4S)$ decay is suppressed for some reason. We will make comments on this later.

Figure 1 is computed under this assumption and this model is called the QPC model. Above 11.10 GeV we have not tried to fit the data since we are neglecting $B_p\bar{B}, B_p\bar{B}^*$, etc. ($B_p \equiv 1P$, $b\bar{u}$ state), channels.

2. QHM model

We now consider the reason why the decay of $\Upsilon(4S)$ is suppressed. Let us briefly summarize the value of $\gamma_{\rm QPC}$ used for various processes. For light-quarkonium decay $\gamma_{\rm QPC}=4.7$ was used by Ono and Pène[25] and for charmonium we need $\gamma_{\rm QPC}=3.43$ ($=2.2\times 2\sqrt{6}/\pi$ in the normalization of Ref. 25) without unitarity effects or $\gamma_{\rm QPC}=3.029$ with unitary effects. $\gamma_{\rm QPC}$ is supposed to be a universal flavor-independent coupling constant.

Let us show that if we take into account the mixing between the hybrid states ($Q\bar{Q}g$) and the quarkonium states ($Q\bar{Q}$) the inconsistency in $\gamma_{\rm QPC}$ can become systematically small.

As for light-quarkonium decays only ground states ($1S$) are considered. Hybrid states are much heavier than ground states, thus hybrid-quarkonium mixing is negligible for these states. Thus, the obtained value $\gamma_{\rm QPC}=4.7$ can be used as a standard value.

Let us carefully check the results of Ref. 13 where $\gamma_{\rm QPC}=3.029$ is found from $c\bar{c}$ and $b\bar{b}$ data. Predicted widths are[13]

	Mass (GeV)	Width Expt (MeV)	Theory (MeV)
$\psi(1D)$	3770	25±3	10.9
$\psi(3S)$	4030	52±10	60.1
$\psi(2D)$	4159	78±20	71.5
$\psi(4S)$	4415	43±20	19.6

(A1)

As shown in Sec. III the anomaly in $\Gamma_{ee}(2D)/\Gamma_{ee}(3S)$ can be solved if we assume $\psi(4030)$ and $\psi(4159)$ are mixture states between $c\bar{c}g$ and $(c\bar{c})_{3S}$ [see Eq. (3.2)]. By using exactly the same mechanism we can also solve problems in OZI-rule-allowed decay widths. Let us increase $\gamma_{\rm QPC}$ from 3.029 to 4.5 (this is nearer to the 4.7 found for the light-quarkonium decay). By multiplying $(4.5/3.029)^2$ we can estimate the widths for c.c. states. Because of the selection rule found by Le Yaouance *et al.*[26] this $c\bar{c}g$ state cannot decay into $D\bar{D}, D\bar{D}^*$+c.c., etc.; thus, the widths for $\psi(4030)$ and $\psi(4159)$ are just one-half of the $(c\bar{c})_{3S}$ with [see Eq. (3.2) and the following discussions]. Thus, one finds (in MeV, numbers in parentheses are experimental ones)

$$\begin{aligned}
\Gamma(3770) &= 10.9\times(4.5/3.029)^2 \\
&= 24.1\ (25\pm 3)\ , \\
\Gamma(4030) &= 60.1\times(4.5/3.029)^2/2 \\
&= 66\ (52\pm 10)\ , \\
\Gamma(4159) &= 66(78\pm 20)\ , \\
\Gamma(4415) &= 43(43\pm 20)\ ,
\end{aligned} \tag{A2}$$

which are in an excellent agreement with the data.

We will now show that exactly the same mechanism solves the following anomalies in $b\bar{b}$.

(i) The mass of $\Upsilon(4S)$ is abnormally low. This can be easily seen from the observed relation $M(5S)-M(4S) > M(4S)-M(3S)$.

(ii) $\Gamma_{ee}(4S)$ is smaller than theoretically expected and even smaller than $\Gamma_{ee}(5S)$.

This situation is unacceptable in any potential model but can easily be explained in the $b\bar{b}$-$b\bar{b}g$ mixing model.

Theoretically the width of $\Upsilon(4S)$ is 19.8 MeV for $\gamma_{\rm QPC}=3.029$ (see comment of Table IV in Ref. 13) and 43.7 MeV for $\gamma_{\rm QPC}=4.5$ while 25±2.5 (CUSB[8]) and 20±6 MeV (CLEO[9]) are found experimentally. If we set $\gamma_{\rm QPC}=4.5$ and assume that 40% of $b\bar{b}$ component in $\Upsilon(4S)$ is taken away due to $b\bar{b}$-$b\bar{b}g$ mixing, then we find $\Gamma(4S)=26$ MeV, which is consistent with the data.

We now assume that there is a mixing partner to $\Upsilon(4S)$ at 10.684 GeV, i.e., just above $\Upsilon(4S)$ and the ratio of the $b\bar{b}$ component inside Υ''' and that of the mixing partner [$\Upsilon(10684)$] is five to four. We neglect the $\Upsilon(5S)$ component in $\Upsilon(10684)$ since a model calculation shows it is small. Figure 2 is computed under this assumption.

Can one understand why we need a rather large $\gamma_{\rm QPC}$ (=5.6) for resonances above $5S$? We should point out that it is also possible to find a good fit with smaller $\gamma_{\rm QPC}$ if the background level is increased and the e^+e^- coupling decreased. In the present fit we have used the background level 4.5 which was determined below threshold (see Ref. 27). In this sense our fitting procedure is similar to the one by the CUSB group.[8] On the other hand if we use the higher background level like the CLEO analysis,[9] we will find a good fit with smaller resonance widths, i.e., smaller $\gamma_{\rm QPC}$ values. One can see, for example, that $\Gamma_{ee}(5S)$ found by CLEO[9] (=0.37 keV) is indeed smaller than that by CUSB[8] (=0.22 keV). In this sense the inconsistency in $\gamma_{\rm QPC}$ is not so serious as it appears.

3. Discussion of UQM results and parameters

The fit to the ratio R shown in Fig. 12(a) uses for the resonances up to $5S$ the same parameters as in the previously published work[15] [a universal $\gamma_{\rm QPC}=3.029$, (bare) resonance masses and bare e^+e^- couplings taken from experiment or potential model]. We were able to fit the $4S$ and $5S$ widths with the same $\gamma_{\rm QPC}$ because the mixing correctly reduces the naive $4S$ width but increases the $5S$ width. The structure seen between the $4S$ and $5S$ is not due to resonances in the UQM, but comes from the interplay of opening of new channels followed by nodes in the spatial overlaps in $\langle i \mid H_{\rm QPC} \mid B\bar{B}^* \rangle$ and $\langle i \mid H_{\rm QPC} \mid B^*\bar{B}^* \rangle$.

The $3D$ state which is expected to lie in this region was included in the model as well as other D states and could in principle contribute through mixing with the S-wave states. We found, however, this mixing to be too small to account for the structure seen. The model thus does predict a "background" which comes partly from all the other resonances (altogether 7 S states and 6 D states were included) and partly from the non-Breit-Wigner shapes of the resonances. However, this background may be still too small since we needed a constant 4.8 instead of 4.5 expected from the background below threshold. Thus without further increasing the e^+e^- couplings and the $\gamma_{\rm QPC}$ parameter there is room for new physics like hybrid $Q\bar{Q}g$ states or a nonresonant background.

For the $6S$ (and $7S$) resonances the model without new parameters predicts states which are too narrow. This is due to the fact that our nodes of the overlap functions are rather close to the resonance position and that the UQM mixing now works in the wrong direction decreasing further the widths. As discussed in Sec. IV the real parts of the off-diagonal matrix elements are sensitive to the details of the QPC model. Thus to get a good fit to the $6S$ and $7S$ states we put the $\mathrm{Re}M_{ij}{}^2(s)$, $i\neq j$ involving these high resonances zero by hand, and increased $\gamma_{\rm QPC}$ by a factor $\sqrt{2}$ for these states ($\gamma_{\rm QPC}=4.289$). Of course this does not violate the unitarity condition [Eq. (4.4)], it only reflects the uncertainty inherent in the far-off-shell dependence of the QPC model.

In summary the other parameters of the calculation and the computed mass shifts are given in Table I. In particular, the $5S$-$4S$ splitting, anomalously larger than the $4S$-$3S$ splitting, can be understood because of these hadronic mass shifts as already emphasized in Ref. 15.

APPENDIX B: COMMENTS ON $B^0\bar{B}^0/B^+B^-$ RATIO ON $\Upsilon(4S)$

Experimentally $\Upsilon(4S)$ is known to be just above $B\bar{B}$ threshold:

$$\Upsilon(4S)-2B=31.7\pm2.9\pm4.0\ \text{GeV}\ . \tag{B1}$$

The masses of B^0 and $B^\pm$ are found by reconstructing $B\to D+n\pi$ events:

$$B^0-B^-=4.0\pm2.7\pm2.0\ \text{MeV}\ . \tag{B2}$$

Using the decay width formula for P-wave decay near threshold

$$\Gamma\propto p^3 \tag{B3}$$

and assuming $B^0-B^\pm=4.4$ MeV and $\Upsilon(4S)-2B=30$ MeV one finds

$$\begin{aligned} &B(\Upsilon(4S)\to B^0\bar{B}^0)\simeq0.40\ ,\\ &B(\Upsilon(4S)\to B^+B^-)\simeq0.60\ . \end{aligned} \tag{B4}$$

However, one must remember that Eq. (B4) holds only for small p. In our case $\Upsilon(4S)$ is 30 MeV above threshold; that is, the decay momentum is as large as $p\approx400$ MeV. The overlap integral in the decay amplitude is a rapidly oscillating function. Explicit calculation in the QPC model shows $\Gamma_{\Upsilon'''\to B\bar{B}}(p)$ reaches the local maximum at around $p\sim400$ MeV and it has the first node at $p\sim750$ MeV. This means $\Upsilon(4S)$ is already too far from the threshold to use the relation $\Gamma\propto p^{2l+1}$. Since it is near the local maximum the small difference in the phase space between $B^0\bar{B}^0$ and B^+B^- does not affect the branching ratio much.

Assuming $\Upsilon(4S)-2B=31.1$ MeV and $B^\pm=B+\delta$, $B^0=B-\delta$ we compute the ratio $r\equiv B(\Upsilon(4S)\to B^+B^-)/B(\Upsilon(4S)\to B^0\bar{B}^0)$ at the top of the resonance by using the QPC model. We find $r=0.4984/0.5016$ for $B^0-B^\pm=4$ MeV which is much different from (B4). Since the difference $B^0-B^\pm$ is not precisely known experimentally, we compute r for various δ:

$$\begin{aligned} &r=0.4995/0.5005 \ \text{for}\ B^0-B^\pm=2\ \text{MeV}\ ,\\ &r=0.4984/0.5016 \ \text{for}\ B^0-B^\pm=4\ \text{MeV}\ ,\\ &r=0.4967/0.5033 \ \text{for}\ B^0-B^\pm=6\ \text{MeV}\ ,\\ &r=0.4896/0.5104 \ \text{for}\ B^0-B^\pm=8\ \text{MeV}\ . \end{aligned} \tag{B5}$$

As seen from this calculation the assumption $B(\Upsilon(4S)\to B^+B^-)=B(\Upsilon(4S)\to B^0\bar{B}^0)=0.5$ is always

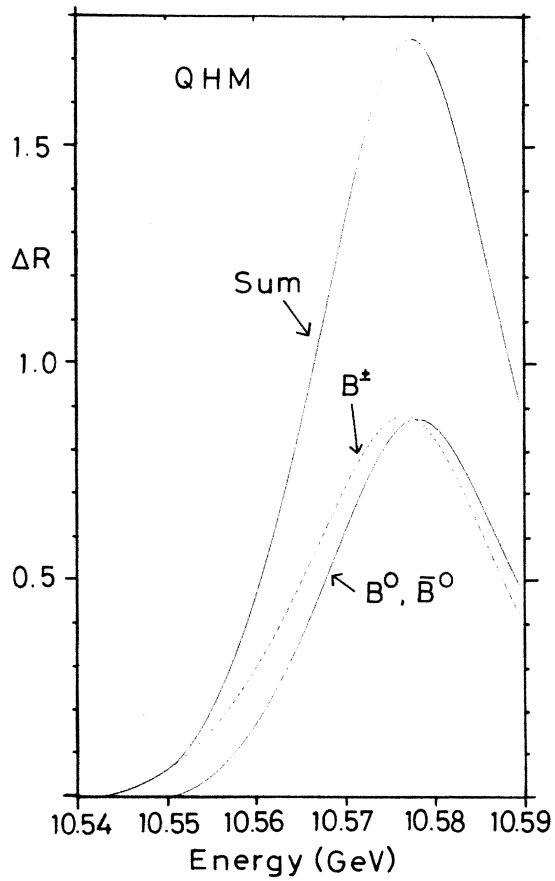

FIG. 13. The contribution to R from $B^0\bar{B}^0$ and $B^+\bar{B}^-$ as predicted by QHM with $\Delta m_{\rm EM}\equiv B^0-B^\pm=4$ MeV.

much better than (B4) for any reasonable values of $B^0-B^{\pm}$. As a typical example we show ΔR contributions of B^0 and $B^{\pm}$ from $\Upsilon(4S)$ for $B^0-B^{\pm}=4$ meV in Fig. 13. In the present paper we have always used the assumption $B(\Upsilon(4S)\to B^0\bar{B}^0)=B(\Upsilon(4S)\to B^+B^-)$.

APPENDIX C: OBSERVABILITY OF *CP* VIOLATION IN THE B-$\bar{B}$ SYSTEM

The parameters for *CP* violation can be expressed by the asymmetry in the same-sign dilepton events:

$$A\equiv\frac{\sigma^{++}-\sigma^{--}}{\sigma^{++}+\sigma^{--}}=\mathrm{Im}\left[\frac{\Gamma_{12}}{M_{12}}\right]. \tag{C1}$$

Unfortunately, this is very small, $\sim 10^{-4}$ both for $B_d\bar{B}_d$ and $B_s\bar{B}_s$ and very difficult to observe. It was shown[28] that this asymmetry parameter for $B_s\bar{B}_s$ is very sensitive to new physics such as supersymmetry, since it adds a large term with a different phase in the denominator:

$$\mathrm{Im}\left[\frac{M_{12}^{\mathrm{KM}}e^{i\phi}}{M_{12}^{\mathrm{KM}}e^{i\phi}+M_{12}^{\mathrm{new}}}\right] \tag{C2}$$

which could be as large as $\sim 10^{-2}$ (M_{12}^{KM} is an element of the Kobayashi-Maskawa matrix). Since there is no such enhancement for B_d-$\bar{B}_d$ mixing, the best place to sit is again the $\Upsilon(5S)$ region.

---

*Present address: Physics Department, University of Tokyo, Tokyo 113, Japan.

[1]J. K. Black *et al.*, Phys. Rev. Lett. **54**, 1628 (1985); R. H. Bernstein *et al.*, *ibid.* **54**, 1631 (1985).

[2]By the standard model we mean SU(2)×U(1) electroweak gauge theory with a weak mixing angle governed by the Kobayashi-Maskawa matrix.

[3]A. Pais and S. B. Treiman, Phys. Rev. D **12**, 2744 (1975); L. B. Okun, V. I. Zakharov, and B. M. Pontecorvo, Lett. Nuovo Cimento **13**, 218 (1975); J. Ellis, M. K. Gaillard, and D. V. Nanopoulos, Nucl. Phys. **B109**, 213 (1976); A. Ali and Z. Z. Aydin, *ibid.* **B148**, 165 (1978).

[4]A. B. Carter and A. I. Sanda, Phys. Rev. D **23**, 1567 (1981); I. I. Bigi and A. I. Sanda, Nucl. Phys. **B193**, 123 (1981); Comments Nucl. Part. Phys. **14**, 149 (1985).

[5]J. Lee-Franzini, in $B^0\bar{B}^0$ *Mixing,* proceedings of the Fifth Moriond Workshop, La Plagne, France, 1985, edited by J. Tran Thanh Van (Editions Frontières, Gif-sur-Yvette, 1985).

[6]S. Ono, A. I. Sanda, N. A. Törnqvist, and J. Lee-Franzini, Phys. Rev. Lett. **55**, 2938 (1985).

[7]D. Loveless *et al.*, in *Proceedings of DPF workshop on $\bar{p}p$ Options for the Super Collider, Chicago, 1984.* edited by J. Plicher and A. R. White (Physics Department, University of Chicago, Chicago, 1984).

[8]D. M. J. Lovelock *et al.*, Phys. Rev. Lett. **54**, 377 (1985).

[9]D. Besson *et al.*, Phys. Rev. Lett. **54**, 381 (1985).

[10]S. Ono, Orsay, Report No. LPTHE 83/32, 1983 (unpublished).

[11]S. Ono, Z. Phys. C **26**, 307 (1985).

[12]S. Ono, in *Proceedings of the XIXth Rencontre de Moriond, La Plagne, France, 1984,* edited by J. Tran Thanh Van (Editions Frontières, Gif-sur-Yvette, 1984); and Ref. 5.

[13]K. Heikkilä, S. Ono, and N. A. Törnqvist, Phys. Rev. D **29**, 110 (1984).

[14]N. A. Törnqvist, Acta Phys. Pol. **B16**, 503 (1985).

[15]N. A. Törnqvist, Phys. Rev. Lett. **53**, 878 (1984).

[16]A. J. Buras, W. Slominski, and H. Steger, Nucl. Phys. **B245**, 369 (1984); see also M. B. Gavela *et al.*, Phys. Lett. **154B**, 147 (1985); I. I. Bigi, Aachen Report No. PITHA 85/10, 1985 (unpubished). For bag parameters β_s and β_d see I. I. Bigi and A. I. Sanda Phys. Rev. D **29**, 1393 (1984); and also F. Wagner, Report No. MPI PAE PTH 89/83 (unpublished). In the latter reference Wagner discusses the possibility that β is larger than the value predicted by conventional potential models.

[17]A. Le Yaouanc, L. Oliver, O. Pène, and J.-C. Raynal, Phys. Rev. D **8**, 2223 (1973).

[18]I. I. Bigi and S. Ono, Nucl. Phys. **B189**, 229 (1981).

[19]P. Hasenfratz *et al.*, Phys. Lett. **22B**, 299 (1980).

[20]T. Kitazoe *et al.*, Z. Phys. C **24**, 143 (1984).

[21]L. J. Reinders, in Proceedings of the 1985 Europhysics Conference on High Energy Physics, Bari, Italy, edited by L. Nitti and G. Preparata (unpublished).

[22]K. Han *et al.*, Phys. Rev. Lett. **55**, 36 (1985).

[23]C. Mahaux and H. A. Wiedenmuller, *Shell Model Approach to Nuclear Reactions* (North-Holland, Amsterdam, 1969).

[24]E. Eichten, Phys. Rev. D **22**, 1819 (1980); E. Eichten *et al.*, *ibid.* **17**, 3090 (1978).

[25]S. Ono and O. Pène, Z. Phys. C **21**, 109 (1983).

[26]A. Le Yaouanc, L. Oliver, S. Ono, O. Pène, and J.-C. Raynal, Z. Phys. C **28**, 309 (1985).

[27]E. Rice *et al.*, Phys. Rev. Lett. **48**, 906 (1982).

[28]A. I. Sanda, Rockefeller University Report No. RU86/B/119, 1985 (unpublished).